The endothelial adrenomedullin-RAMP2 system regulates vascular integrity and suppresses tumor metastasis

Megumu Tanaka[a], Teruhide Koyama[a], Takayuki Sakurai[a], Akiko Kamiyoshi[a], Yuka Ichikawa-Shindo[a], Hisaka Kawate[a], Tian Liu[a], Xian Xian[a], Akira Imai[a], Liuyu Zhai[a], Kazutaka Hirabayashi[a], Shinji Owa[a], Akihiro Yamauchi[a], Kyoko Igarashi[a], Shun'ichiro Taniguchi[b], and Takayuki Shindo[a]

[a]Department of Cardiovascular Research, Shinshu University Graduate School of Medicine, Japan

[b]Department of Molecular Oncology, Shinshu University Graduate School of Medicine, Japan

Contribution

M.T., T.K., S.T., T.SH. conceived and designed the research; T.SA., A.K., Y.I-S., H.K., analyzed and interpreted the data; T.L., X.X., A.I, L.Z., K.H., S.O., A.Y., K.I acquired data.

Word Count 6,970

Address for correspondence: Takayuki Shindo, MD, PhD, Department of Cardiovascular Research, Shinshu University Graduate School of Medicine, Asahi 3-1-1, Matsumoto, Nagano, 390-8621, Japan. Tel: +81-263-37-2578, Fax: +81-263-37-3437, Email: tshindo@shinshu-u.ac.jp

Abstract

Aims- Controlling vascular integrity is expected to be a novel therapeutic target of cancers as well as cardiovascular diseases. Adrenomedullin (AM) and its receptor-modulating protein, RAMP2, have been identified as essential mediators of cardiovascular homeostasis. In this study, we used inducible vascular endothelial cell-specific RAMP2 knockout (DI-E-RAMP2-/-) mice to clarify the contribution made by the endogenous AM-RAMP2 system to angiogenesis and metastasis.

Methods and Results- Subcutaneously transplanted sarcoma or melanoma cells showed less growth and angiogenesis in DI-E-RAMP2-/- than control mice. On the other hand, after transplantation of B16BL6 melanoma cells into hindlimb footpads, spontaneous metastasis to the lung was enhanced in DI-E-RAMP2-/- mice. Early after RAMP2 gene deletion, DI-E-RAMP2-/- mice showed enhanced vascular permeability, endothelial-mesenchymal transition (EndMT)-like change, and systemic edema. Within the lungs of DI-E-RAMP2-/- mice, pulmonary endothelial cells were deformed, and inflammatory cells infiltrated the vessel walls and expressed the chemotactic factors S100A8/9 and SAA3, which attract tumor cells and mediate formation of a pre-metastatic niche. Conversely, overexpression of RAMP2 suppressed tumor cell adhesion to endothelial cells, tumor metastasis, and improved survival.

Conclusions- These findings indicate that the AM-RAMP2 system regulates vascular integrity, whereas RAMP2 deletion promotes vascular permeability and EndMT-like change within primary lesions and formation of pre-metastatic niches in distant organs by destabilizing the vascular structure and inducing inflammation. Vascular integrity regulated by the AM-RAMP2 system could thus be a hopeful therapeutic target for suppressing tumor metastasis.

Introduction

Under normal physiological conditions, angiogenesis occurs primarily during fetal development, in response to ovulation, and during wound healing. The newly developed vascular structures are lined with endothelial cells that integrate functionally into the organ, thereby mediating tissue growth and development [1, 2]. In contrast, pathological angiogenesis has been implicated in many diseases, including cancer and chronic inflammatory diseases [3]. In cancer, pathological angiogenesis promotes the uncontrolled proliferation of tumor cells and supports tumor invasion and metastasis. Therefore, controlling vascular integrity is a promising potential therapeutic target of cancers.

Adrenomedullin (AM) is a bioactive peptide first identified in human pheochromocytoma [4]. It is now known that AM is secreted broadly in various organs and tissues, especially in the cardiovascular system. AM initially attracted attention as a vasodilating peptide. In subsequent studies, however, AM was shown also to have anti-inflammatory, anti-oxidative, anti-fibrotic properties, among others [5-8]. AM is therefore now recognized to be a pleiotropic molecule involved in both the pathogenesis of cardiovascular diseases as well as circulatory homeostasis. Genetically engineered mice have served as a powerful tool with which to study the functions of AM. We reported that homozygous AM knockout (AM-/-) mice die *in utero* due to abnormalities in their cardiovascular development [9]. From this result, we first found that AM is indispensable for angiogenesis during embryonic development. We later found that AM also exerts important angiogenic effects in adults [10], which suggests AM could be potentially useful for the treatment of cardiovascular diseases [11-14]. On the other hand, in oxygen-induced retinopathy (OIR), pathological angiogenesis is suppressed in heterozygous AM knockout (AM+/-) mice or by intravitreal injection of anti-AM antibody [15]. High levels of AM expression have also been detected in various cancer cell types [16-18]. These observations suggest AM is a potential therapeutic target for controlling pathological angiogenesis.

AM is a member of the calcitonin superfamily and acts via a G protein-coupled seven transmembrane domain receptor, calcitonin-receptor-like receptor (CLR) [19, 20]. The specificity

of CLR for its ligands is determined by three receptor-activity-modifying proteins, RAMP1, -2 and -3. We showed that homozygous RAMP2 knockout (RAMP2-/-) mice exhibit an embryonically lethal phenotype with abnormal vascular development that is nearly identical to that of AM-/- mice [21]. Thus, deletion of RAMP2 almost entirely reproduces the major phenotypes of AM-/-, suggesting RAMP2 is specifically involved in the cardiovascular function of AM.

We have been focusing on RAMP2 as an alternative therapeutic target for AM, since we are able to modulate the cardiovascular functions of AM by modulating RAMP2. For example, we established vascular endothelial cell-specific RAMP2 conditional knockout mice (E-RAMP2-/-). But although E-RAMP2-/- mice survive longer than RAMP2-/- mice, most died of endothelial abnormality and vascular leakage during the perinatal period [22], limiting their utility. We therefore next generated a drug-inducible endothelial cell-specific RAMP2 knockout mouse (DI-E-RAMP2-/-). With this model, fetal death was avoided, and we were able to induce vascular endothelial cell-specific RAMP2 gene deletion in adult animals.

When considering cancer therapy through intervention via the vascular system, its side effects on vascular integrity and homeostasis become another important issue. Clinical and preclinical investigations have identified major drawbacks associated with the application of anti-angiogenic agents for cancer treatment. For example, inhibitors of the VEGF pathway exhibit antitumor effects but also heighten the invasiveness of tumor cells and increase distant metastasis [23, 24]. Clearly, for the development of new therapies targeting vasoactive molecules, we will need to know more about the mechanisms responsible for the maintenance of vascular integrity. By utilizing DI-E-RAMP2-/- mice, in this study we for the first time revealed the role of the vascular AM-RAMP2 system in both tumor angiogenesis and metastasis.

Methods

Generation of gene-engineered mice

RAMP2-/- and RAMP2+/- mice were previously generated in our group [21]. Tamoxifen drug-inducible (DI) vascular endothelial cell-specific RAMP2 knockout mice (DI-E-RAMP2-/-) were generated by crossbreeding mice expressing tamoxifen-inducible Cre-recombinase (Cre-ERT2) under the control of the vascular endothelial (VE)-cadherin promoter [25] with floxed RAMP2 mice (RAMP2flox/flox). To induce RAMP2 gene-deletion in DI-E-RAMP2-/- mice, tamoxifen (Sigma) was dissolved in corn oil (Sigma) to a concentration of 10 mg/ml, after which 1 mg was intraperitoneally injected into 8 week-old male mice daily for 5 days. Little toxicity was observed following the injection into wild-type (WT), RAMP2 flox/flox, or Cre-ERT2 mice.

Endothelial cell-specific RAMP2-overexpressing transgenic (E-RAMP2 Tg) mice were generated by microinjection of plasmid DNA constructed for overexpression of RAMP2 under the control of the VE-cadherin promoter. Mouse open reading frame cDNA was inserted into a plasmid containing a 2.53 kb 5'-flanking region of the mouse VE-cadherin gene and a rabbit β-globin poly-A signal. In the present study, primary-cultured pulmonary endothelial cells from the transgenic mouse line expressed over 100 higher RAMP2 levels than corresponding cells from WT mice. Survival time after the transplantation of B16BL6 melanoma cells was analyzed in E-RAMP2 Tg (n = 7) and WT mice (n = 8).

The background of all the mice used in this study was C57BL/6J.

All animal handling procedures were performed in accordance with protocols approved by the Ethics Committee of Institutional Animal Care and Use Committee and NIH guidelines (Guide for the care and use of laboratory animals).

Tumor cell transplantation

Before the subcutaneous injection, mice skins were locally anesthetized using 2% lidocaine

hydrochloride jelly. Sarcoma 180 (S180) murine transplantable tumor cells (2×10^6 cells in 0.2 ml of vehicle) were transplanted subcutaneously into the bilateral axillary regions of each mouse [10]. n = 11 in both groups. B16F10 melanoma (B16F10) cells (1×10^5 cells in 0.2 mL of vehicle) were transplanted subcutaneously into the axillary region on one side in each mouse. n = 10 for control and n = 8 for DI-E-RAMP2-/-.

Before the operative procedures, mice were anesthetized by intraperitoneal injection of 2,2,2-tribromoethanol (240 mg/kg; Wako, Osaka, Japan). Three weeks after the transplantation, histological studies were performed for analysis of the primary lesions. n = 8 to 10. In addition, B16BL6 melanoma cells (B16BL6), which are prone to metastasis to distant organs, were used to analyze spontaneous lung metastasis in this study. B16BL6 cells (1.5×10^4 cells in 0.05 mL of vehicle) were transplanted subcutaneously into a foot-pad of each mouse [26]. n = 12 to 13. After 3 weeks, under anesthesia using intraperitoneal injection of 2,2,2-tribromoethanol (240 mg/kg), the transplanted foot was amputated. After an additional 4 weeks, after anesthesia by intraperitoneal injection of 2,2,2-tribromoethanol (240 mg/kg), the lungs were removed for analysis of metastasis. B16F10 and B16BL6 cells were cultured and passaged in Dulbecco's modified Eagle's medium (DMEM) (Invitrogen) supplemented with 10% FBS.

Matrigel plug assay

After the mice were anesthetized, 500 μL of Matrigel (BD) containing 100 ng of recombinant human bFGF (Wako, Osaka, Japan) was injected subcutaneously into the dorsal region of mice using a 25-gauge needle [21]. Experiments were repeated 4 times. One week later, the skin around the injected Matrigel was incised, and the angiogenic response was analyzed. Capillaries growing in the Matrigel were stained with anti-CD31 antibody (BD Biosciences) and anti-α-smooth muscle actin antibody (SIGMA).

Cell culture

A RAMP2-overexpressing (RAMP2 O/E) cell line was created using EAhy926 endothelial cells as described previously [21]. EAhy926 endothelial cells were cultured in DMEM containing 10% FBS.

Human umbilical vein endothelial cells (HUVECs) (TOYOBO, Osaka, Japan) were cultured according to the manufacturer's protocol. Ds-Red-expressing B16F10 melanoma cells (B16F10-RFP) were purchased from AntiCancer (Chiba, Japan) and cultured in RPMI-1640 with 10% FBS. HUVECs were also co-cultured with B16F10 melanoma cells isolated from tumors grown over a 2-week period. Experiments were repeated 4 times.

After anesthesia by intraperitoneal injection of 2,2,2-tribromoethanol (240 mg/kg), pulmonary endothelial cells were isolated from 11-week-old DI-E-RAMP2-/- mice and control mice using positive magnetic selection [27]. DI-E-RAMP2-/- mice were used after inducing gene deletion for 3 weeks. Endothelial cells were isolated using an EasySep Biotin Selection Kit protocol (STEMCELL Technologies). Lungs were removed, minced, and digested in collagenase type 1 (Worthington; S4D7301). A single-cell suspension was prepared by passing the digested lungs through a 40-μm cell strainer (BD Biosciences, Falcon). The cells were then incubated with biotinylated anti-CD31 (Mec 13.3) and washed, after which magnetic antibiotin nanoparticles were added. Unlabeled cells were then poured off, and endothelial cells were collected and cultured. Experiments were repeated 4 times.

Histology

Lung and tumor tissues were fixed overnight in 4% paraformaldehyde and embedded in paraffin, after which the lung tissue was cut into 4-μm-thick sections and the tumor tissue was cut into 5-μm-thick sections. The sections were then deparaffinized for hematoxylin/eosin (H&E) and Fontana Masson staining and immunohistochemistry. Immunostaining was performed using anti-CD31 (BD Biosciences), anti-α-smooth muscle actin (SIGMA), anti-fibroblast-specific protein-1 (FSP-1) (MILLIPORE), anti-VE Cadherin (Abcam), anti-F4/80

(Serotec), anti-4-hydroxy-2-nonenal (4HNE) (NOF CORPORATION, Tokyo, Japan), and anti-S100A8 (ABGENT) antibodies.

The sections were then stained with Alexa Fluor 488- or 568-conjugated anti-rabbit, anti-goat, and anti-mouse secondary antibodies (ThermoFisher SCIENTIFIC). To immunostain 4HNE and S100A8, biotin-conjugated secondary antibodies were used. Intracellular actin filaments were stained using rhodamine phalloidin (ThermoFisher SCIENTIFIC), and nuclei were stained using DAPI (ThermoFisher SCIENTIFIC). Fluorescence was observed using a fluorescence microscope equipped with the appropriate filter sets (BZ-900, KEYENCE, Osaka, Japan). Average of 10 microscopic fields per tumor were analyzed.

Quantitative real-time RT-PCR analysis

Quantitative real-time RT-PCR was carried out using an Applied Biosystems 7300 real-time PCR System with SYBR green (Toyobo, Japan) or Realtime PCR Master Mix (Toyobo) and TaqMan probes (MBL, Nagoya, Japan). The primers and probes used are listed in Table. 1. Values were normalized to mouse GAPDH (Pre-Developed TaqMan assay reagents, Applied Biosystems). Sample numbers are shown in each Figure legends.

Transmission electron microscopy

Specimens were fixed in 2.5% glutaraldehyde (pH 7.2), embedded in epoxy resin (Epok) 812 (Oken Shoji, Tokyo, Japan), cut into ultrathin sections, stained with uranyl acete and lead citrate, and examined under an electron microscope. Experiments were repeated 4 times.

Indocyanine green tumor angiography

To visualize tumor vascular structure, 100 μL of indocyanine green (ICG) (Daiichi-Sankyo, Tokyo, Japan) was intraperitoneally injected into the mice 2 weeks after transplantation of the B16F10 melanoma cells. Thirty minutes after ICG administration, images were taken using a Heidelberg Retina Angiograph 2. Experiments were repeated 4 times.

Statistical analysis

Values are expressed as means ± SEM. Student's t test or $\chi 2$-test was used to evaluate the significance of differences. Values of $P < 0.05$ were considered significant.

Results

Tumor angiogenesis and growth were suppressed in DI-E-RAMP2-/- mice

Using tumor transplantation models with DI-E-RAMP2-/- mice and control mice, we analyzed the effects of deleting the RAMP2 gene from vascular endothelial cells on tumor angiogenesis and growth. Macroscopic observation of the excised sarcoma 180 tumors showed poor vascular development (Fig. 1A) and significantly reduced tumor weight in DI-E-RAMP2-/- compared to control mice (Fig. 1C, left). In the transplantation of B16F10 melanoma cells, tumor weights were again significantly lower in DI-E-RAMP2-/- than control mice (Fig. 1C, right). Interestingly, B16F10 melanoma tumors excised from DI-E-RAMP2-/- mice showed signs of self-destruction (Fig. 1B). We thought that the self-destruction of the transplanted tumor was triggered by a lack of blood flow due to poor angiogenesis. This idea was confirmed by the observation that capillarization within B16F10 melanomas was significantly diminished in DI-E-RAMP2-/- mice (Fig. 1D, E). In addition, gene expression of the angiogenic markers CD31, VEGF-A, and VEGFR-2 showed tendency of downregulation in B16F10 melanomas from DI-E-RAMP2-/- mice (Fig. 1F).

Based on the results summarized above, we next performed Matrigel plug assays to more clearly visualize the altered angiogenic potency in DI-E-RAMP2-/- mice. As in the tumors, vascularization of the transplanted Matrigel was much poorer in DI-E-RAMP2-/- than control mice (Fig. 1G). In addition, fluorescent immunostaining of Matrigel sections showed hypoplasia of the tip cells in the elongating vascular front, which may partially explain the reduced angiogenesis in DI-E-RAMP2-/- mice (Fig. 1H). These data suggest that RAMP2 plays a critical role in the vascularization of primary cancers and that RAMP2-deletion suppresses

tumor growth.

Enhanced metastasis in DI-E-RAMP2-/- mice

B16BL6 melanoma cells were established from B16F10 melanoma cells that penetrated the mouse bladder membrane. Although B16F10 and B16BL6 melanoma cells are both malignant and have similar characteristics, B16BL6 melanoma cells implanted into the subcutis are capable of spontaneously metastasizing to the lung, whereas B16F10 melanoma cells colonize in the lung only by direct inoculation into the blood[28]. To assess the effect of RAMP2 deletion on tumor metastasis, B16BL6 melanoma cells were transplanted into the hindlimb footpads of DI-E-RAMP2-/- mice and control mice, and 3 weeks later the primary lesions were resected. Spontaneous lung metastasis was then analyzed 4 weeks after resection of the primary tumor. Contrary to our expectation, the incidence of metastasis and the number of metastatic lesions were higher in DI-E-RAMP2-/- mice than control mice (Fig. 2A, B, C). Metastasis was also confirmed in lung sections using Fontana Masson staining, which reveals the presence of melanin pigment (Fig. 2D).

Vascular abnormalities in primary lesions in DI-E-RAMP2-/- mice

DI-E-RAMP2-/- mice developed systemic edema (Fig. 3A) and increased body weight following gene deletion at day 8 (Fig. 3B left). The systemic edema was likely caused by increased vascular permeability, and was enhanced after transplantation of B16F10 melanoma at day 20 (Fig. 3B right). The survival rate at day 20 was not different between control and DI-E-RAMP2-/- (5 of 8 mice survived), so we thought that the survival rate did not effect on the body weight. We thought that the edema was the primary cause of increased body weight, since we observed the body weight gain even without tumor transplantation in DI-E-RAMP2-/- [22]. Moreover, tumor growth itself was lower in DI-E-RAMP2-/-, however, these mice showed increased body weight.

To further clarify the mechanism by which metastasis is enhanced in DI-E-RAMP2-/-

mice, we used ICG imaging to examine the structure of the vessels within the primary subcutaneously transplanted B16F10 melanoma tumors. We found that vascular narrowing and irregularity with coiling were prominent in DI-E-RAMP2-/- mice (Fig. 3C). Electron microscopic observation of the vessels within tumors in DI-E-RAMP2-/- mice revealed the endothelial cells to be fragile and thin, and the walls partially fragmented, making the vessels leaky (Fig. 3D). In DI-E-RAMP2-/-, abnormal endothelial cells were also observed in various vessels outside of the tumor. In particular, in the kidney, the endothelial side of the glomerular loop showed peculiar change; it looks like honeycomb composed of multilayers of endothelial cells (Fig. 3E). Endothelial cell detachment was also detected in aorta (Supplementary Figure 1). Therefore, RAMP2 deletion caused structural abnormality of various vascular endothelial cells.

In addition, TUNEL-positive apoptotic areas detected in regions distant from the vascular lumen were much larger in the tumor of DI-E-RAMP2-/- mice than control mice (Fig. 3F, G). This may be the result of poor oxygen and nutrient supply through the immature tumor vascular in DI-E-RAMP2-/- mice.

Endothelial-mesenchymal transition (EndMT) was enhanced in DI-E-RAMP2-/- mice.

Endothelial-mesenchymal transition (EndMT) has recently attracted attention as a phenomenon associated with tumor cell intravasation and metastasis[29]. By immunostaining of primary B16F10 melanoma lesions, we detected abnormal growth of α-smooth muscle actin (αSMA)-positive mesenchymal cells within vascular walls in DI-E-RAMP2-/- mice, whereas the numbers of CD31-positive endothelial cells were decreased, which strongly suggests the occurrence of an EndMT-like change (Fig. 4A). In Fontana Masson staining of the primary lesion, which selectively visualizes melanoma cells, we could not detect the staining of cells at the vascular walls (Supplementary Fig. 2.), which indicates that melanoma cells most likely did not transform into endothelial-like cells. We speculated that tumor cells transplanted into DI-E-

RAMP2-/- mice create a microenvironment that alters the characteristics of vascular endothelial cells. To test that idea, we co-cultured HUVECs with primary B16F10 melanoma cells collected from tumors in DI-E-RAMP2-/- or control mice. HUVECs co-cultured with B16F10 melanoma cells from DI-E-RAMP2-/- mice exhibited enhanced actin stress fiber formation (Fig. 4B), which is another characteristic of EndMT. In cultured HUVECs, TGF-β reduced the distribution of VE-cadherin at the cellular membrane and increased actin stress fiber formation, indicating EndMT occurred (Fig. 4C center). Pretreating the cells with AM antagonized the effect of TGF-β, reversing the loss of VE-cadherin from the cellular membrane and the stress fiber formation (Fig. 4C, right). Thus, whereas EndMT-like change is enhanced by AM-RAMP2 deletion, it is suppressed by treating cells with exogenous AM.

To further confirm that RAMP2 gene deletion enhanced the EndMT-like change, we isolated vascular endothelial cells from DI-E-RAMP2-/- and control mice and then assayed EndMT induced by TGF-β *in vitro*. Our findings confirmed that among VE-cadherin-positive endothelial cells, cells also positive for fibroblast-specific protein-1 (FSP-1), a mesenchymal cell marker, were greatly increased in DI-E-RAMP2-/- mice as compared to control mice (Fig. 4D, E).

Evaluation of pre-metastatic niche formation in the lung after RAMP2 deletion

Recently, it is suggested that a favorable environment within a distant organ increases the likelihood that cancer metastasis will occur. This is the so-called pre-metastatic niche[30-32]. We speculated that changes to the lung vasculature caused by RAMP2 deletion leads to formation of a pre-metastatic niche. After inducing RAMP2 gene deletion for 26 days, the lungs of DI-E-RAMP2-/- mice showed interstitial edema (Fig. 5A). Electron microscopic observation revealed the pulmonary endothelial cells in DI-E-RAMP2-/- mice to be deformed and to extend into the vascular lumen (Fig. 5B). Endothelial RAMP2 deletion also suppressed pulmonary VE-cadherin and actin expression (Fig. 5C).

Moreover, we detected prominent invasion of the lungs by macrophages, which were detected mainly along vascular lumens, in DI-E-RAMP2-/- mice (Fig. 6A). In addition, oxidative stress indicated by the accumulation of 4HNE, an unsaturated fatty acid peroxide, was enhanced in the lungs of DI-E-RAMP2-/- mice (Fig. 6B). Correspondingly, greater upregulation of inflammatory cytokines and NADPH oxidase subunits was detected in the lungs of DI-E-RAMP2-/- (Fig. 6C).

Recently, S100A8 and S100A9 have been identified as tumor chemoattractant factors enhancing tumor metastasis to distant organs[30, 31], and their expression was elevated in the lungs of DI-E-RAMP2-/- mice (Fig. 6D, E). In a microarray analysis of mRNA from lung, we found that serum amyloid A (SAA)3, the downstream target of S100A8/9, was strongly upregulated in DI-E-RAMP2-/- mice (Table. 2), and this was confirmed by real-time PCR analysis (Supplementary Fig. 3A). Interestingly, in DI-E-RAMP2-/- x RAMP2+/- crossbred double knockout mice, the upregulation of SAA3 was even more prominent (Supplementary Fig. 3B).

These observations indicate that RAMP2 deletion from vascular endothelial cells enhances pre-metastatic niche formation in the lung, through invasion of the vasculature by inflammatory cells with increases in oxidative stress, and production of tumor chemoattractant factors.

Endothelial RAMP2-overexpression suppresses tumor metastasis

Next, we used EAhy926 endothelial cells to establish an endothelial cell line stably overexpressing RAMP2 (RAMP2 O/E) and then analyzed the adhesion of Ds-Red expressing B16F10 melanoma cells to monolayers of cultured RAMP2 O/E and control endothelial cells. We found that tumor cell adhesion was significantly suppressed in RAMP2 O/E endothelial cells as compared to control cells (Fig. 7A, B).

Finally, to determine whether tumor cell metastasis could be suppressed by stimulating

the AM-RAMP2 system, we generated endothelial cell-specific RAMP2-overexpressing transgenic mice (E-RAMP2 Tg). As expected, after transplantation of B16BL6 melanoma cells into the hindlimb footpads, there was less spontaneous lung metastasis in E-RAMP2 Tg mice than WT mice (Fig. 7C). Moreover, E-RAMP2 Tg mice showed greater survival in a spontaneous lung metastasis model (Fig. 7D).

Discussion

Our findings indicate that deletion of RAMP2 from endothelial cells suppresses growth of locally transplanted tumors by reducing tumor angiogenesis. DI-E-RAMP2-/- mice also showed hypoplasia of the tip cells in Matrigel plug assays. In an earlier tumor transplantation study, we showed that AM upregulates VEGF-A expression in vitro and in vivo [10]. The expression of both VEGF-A and VEGFR-2 was suppressed in melanomas transplanted into DI-E-RAMP2-/- mice. Suppression of VEGF-A/VEGFR-2 signaling could lead to the observed hypoplasia of tip cells in DI-E-RAMP2-/- mice.

We also found that metastasis was exacerbated in DI-E-RAMP2-/- mice. To elucidate the mechanism by which this process is enhanced in DI-E-RAMP2-/- mice, we examined the vascular structure within primary tumors to determine whether it possesses features that would promote metastasis. As we reported previously, DI-E-RAMP2-/- mice showed systemic edema after RAMP2 deletion [22], and this tendency was exacerbated after tumor transplantation in this study. We speculated that cytoskeletal abnormality and disruption of intercellular adhesion of the endothelial cells were the primary causes of the edema. We reported that actin polymerization in DI-E-RAMP2-/- endothelial cells appeared in disarray, and there was a loss of actin-bundle formation under the plasma membrane (cortical actin formation) [22]. It has been reported that small GTPases, Rac1 and RhoA, play crucial roles in the regulation of cell barrier function of endothelial cells by regulating the formation of cortical actin and stress fibers. When we analyzed the activation of Rac1 and RhoA in DI-E-RAMP2-/- endothelial cells, we found that the level of the activated form of Rac1 (Rac1-GTP) was significantly reduced,

whereas the activated form of RhoA (RhoA-GTP) was increased. These observations suggest the AM-RAMP2 system regulates the Rac1-GTP/RhoA-GTP ratio and therefore cortical actin formation, and that a defect in this system will disrupt actin formation and intercellular adhesion of endothelial cells. In this study, we also found pronounced vessel narrowing and irregularity in DI-E-RAMP2-/- mice and observed that the vessel walls were thin and partially fragmented, making the vessels leaky. One difference between tumor angiogenesis and the normal process is that the resulting vessels are tortuous, irregularly shaped, and hyperpermeable, which are hallmarks of pathological angiogenesis [33]. We also found that intraperitoneally injected acridine orange, which is efficiently taken up by malignant tissues, and so is used as a radiation sensitizer, accumulated within tumor tissues more rapidly in DI-E-RAMP2-/- mice than control mice (data not shown). These findings indicate that the dysregulation of tumor vessels was exaggerated in DI-E-RAMP2-/- mice. We also found that, in addition to the tumoral vascular beds, RAMP2 deletion resulted in abnormalities in various vascular endothelial cells, which suggests we should pay attention to the side effects when considering RAMP2 as the therapeutic target. It was reported that AM is also involved in the lymphatic system. Recently, we analyzed which pathways, AM–RAMP2 or AM-RAMP3, is much involved in the lymphatic system[34]. We generated conventional RAMP2 knockout mice, conventional RAMP3 knockout mice, and inducible vascular endothelial-specific RAMP2 knockout mice (used in this study). We used these mice to study tail lymphedema. Following the surgical procedure, the tails of all treated mice became edematous, with the edema reaching a peak on postoperative day 12. As a result, tail thickness was substantially greater in RAMP3-/- mice than in WT mice. We also used the tail lymphedema model in RAMP2+/- and DI-E-RAMP2-/- mice. In contrast to RAMP3-/- mice, the lymphedema of RAMP2+/- and DI-E-RAMP2-/- did not differ from the control mice. In this study, we therefore concentrated on the study of blood vessels.

EndMT has attracted attention as a phenomenon associated with tumor cell intravasation and metastasis [29]. Within primary B16F10 melanomas in DI-E-RAMP2-/- mice, abnormal

overgrowth of αSMA-positive mesenchymal cells in the vascular walls was accompanied by reduced numbers of CD31-positive endothelial cells, which suggests the occurrence of EndMT-like change. Within the tumor microenvironment, endothelial cells lose tight junctions and adhesion molecules, become highly motile, and infiltrate interstitial tissues. Recently, cancer-associated fibroblasts (CAFs) were shown to contribute to cancer progression and metastasis by producing tumor growth factors. Although the origin of CAFs is still being debated, Zeisberg *et al.* reported 30% of the CAFs are generated through EndMT [35]. Cells that have undergone EndMT have also been shown to co-express endothelial and mesenchymal markers [36]. We observed a greater presence of cells positive for both VE-cadherin, an endothelial marker, and FSP-1, a mesenchymal cell marker, in DI-E-RAMP2-/- mice. We also considered the possibility that tumor cells themselves differentiated into endothelial-like cells to generate the vasculature as reported in the case of glioblastoma stem-like cells [37]. However, we did not detect melanoma cells at the vascular walls, which indicates that melanoma cells most likely did not transform into the endothelial-like cells. Glioblastoma stem-like cells form extensive networks of abnormal vasculature characterized by glomeruloid structures and endothelial hyperplasia. Therefore, the situation might not be identical with the melanoma used in our study.

Cancer metastasis depends on the microenvironment in distant organs as well as the primary tumor. This is the so-called pre-metastatic niche [30-32]. We examined the effect of RAMP2 deletion on the formation of a pre-metastatic niche in the lung, and found S100A8/9 expression was elevated in the lungs of DI-E-RAMP2-/- mice. S100A8 and S100A9 are damage-associated molecular pattern molecules (DAMPs), which are secreted from damaged tissues [38] and may act as chemoattractant factors. Hiratsuka *et al.* reported that expression of S100A8 and S100A9 is induced in distant organs prior to metastasis [30, 31], which may enhance the recruitment of tumor cells from the primary lesion.

The vascular deformities and partial detachment of endothelial cells from the vascular wall also likely serve as foci for attachment and invasion of inflammatory cells from the blood stream. In the present study, in DI-E-RAMP2-/- mice we found prominent invasion of inflammatory cells, mainly detected along the pulmonary vessels, as well as upregulation of inflammatory cytokines and enhanced oxidative stress in the lungs. This is consistent with the idea that inflammation is a critical contributor to tumor progression and the fact that many cancers arise from sites of chronic inflammation [39].

We used microarray analysis of lung tissue to compare gene expression in DI-E-RAMP2-/- mice and control mice in an effort to detect other factors that might be involved in formation of the pre-metastatic niche. Among the top 10 upregulated genes in DI-E-RAMP2-/- mice, we focused on SAA3, which in the lung is produced by endothelial cells and inflammatory cells, and is strongly upregulated in DI-E-RAMP2-/- lungs. SAA3 has been shown to be a downstream target of S100A8/9, an endogenous ligand for Toll-like receptor 4 (TLR4), an immune response activator through NF-kB [31], and an important contributor to pre-metastatic niche formation, attracting circulating tumor cells and enhancing lung permeability [32, 40]. In summary, a series of events after the deletion of vascular endothelial RAMP2 may cause the formation of a pre-metastatic niche in the lung, and these distant organ changes promote tumor metastasis in DI-E-RAMP2-/- mice.

Conversely, endothelial cell-specific RAMP2 overexpression in E-RAMP2 Tg mice reduced lung metastasis and promoted survival in a lung metastasis model. We previously reported that stable overexpression of RAMP2 in endothelial cells enhances their barrier function through formation of intercellular tight-junctions [21]. Thus, activation of the AM-RAMP2 system in endothelial cells enhances vascular integrity, which may suppress tumor cell adhesion and invasion.

In this study, we determined that the pathophysiological significance of the AM-RAMP2 system differs between primary tumor growth and metastasis. Fig.8. summarizes our findings on the role of AM-RAMP2 system in tumor angiogenesis and metastasis. AM-RAMP2

suppresses tumor metastasis, while it enhances tumor growth at the primary lesion. This means that caution should be exercised when considering the possible therapeutic applications of AM, as one would not want to promote unfavorable angiogenesis within a primary lesion. However, resection of a primary tumor is often not enough for a cure. To control tumor metastasis, one must consider the systemic vascular integrity within the entire body. This is made apparent by the fact that VEGF inhibitors suppress tumor growth by inhibiting angiogenesis, but also increase invasiveness and the likelihood of distant metastasis. We think that AM has the potential to serve as an adjuvant to suppress metastasis after resection of primary tumors.

Clinical trials of AM for the treatment of inflammatory bowel diseases have been run, as AM exerts anti-inflammatory effects [41]. However, AM is a peptide with a very short half-life in the bloodstream, which limits its usefulness for treatment of chronic diseases. Our focus therefore has been an AM receptor. It is noteworthy that we are able to modulate AM function in the vasculature by modulating RAMP2. RAMP2 could be a useful therapeutic target to suppress metastasis by controlling vascular integrity.

Funding

Supported by Grant-in-Aid for Scientific Research (KAKENHI), the Core Research for Evolutionary Science and Technology (CREST) of Japan Science and Technology Agency (JST) and Japan Agency for Medical Research and Development (AMED), National Cardiovascular Center research grant for cardiovascular diseases, grants-in aid of The Public Trust Fund For Clinical Cancer Research, Mitsui Life Social Welfare Foundation, Takeda Science Foundation research grant, Opto-Science and Technology research grant, Takeda Medical Research Foundation research grant, Elderly eye disease research foundation research grant, Novartis Foundation for Gerontological Research research grant, Cosmetology Research Foundation research grant, SENSHIN Medical Research Foundation research grant, Kanzawa Medical Research Foundation research grant, Ono Medical Research Foundation research grant, the Nakatomi Foundation research grant, Research Foundation for the Japan Vascular Disease Research

Foundation research grant, and Ichiro Kanehara Foundation research grant.

Acknowledgements

The authors thank Dr. K. Kangawa for AM, Dr. C. J. Edgell for EAhy926 cells, and Dr. R. H. Adams for VE-cadherin-Cre-ERT2 mice.

Conflict of interest

None

References

1. Adams RH, Alitalo K. Molecular regulation of angiogenesis and lymphangiogenesis. *Nat Rev Mol Cell Biol* 2007;**8**:464-478.
2. Risau W, Flamme I. Vasculogenesis. *Annu Rev Cell Dev Biol* 1995;**11**:73-91.
3. McDonald DM, Choyke PL. Imaging of angiogenesis: from microscope to clinic. *Nat Med* 2003;**9**:713-725.
4. Kitamura K, Kangawa K, Kawamoto M, Ichiki Y, Nakamura S, Matsuo H, Eto T. Adrenomedullin: a novel hypotensive peptide isolated from human pheochromocytoma. *Biochem Biophys Res Commun* 1993;**192**:553-560.
5. Abe M, Sata M, Nishimatsu H, Nagata D, Suzuki E, Terauchi Y, Kadowaki T, Minamino N, Kangawa K, Matsuo H, Hirata Y, Nagai R. Adrenomedullin augments collateral development in response to acute ischemia. *Biochem. Biophys. Res. Commun.* 2003;**306**:10-15.
6. Brain SD, Grant AD. Vascular actions of calcitonin gene-related peptide and adrenomedullin. *Physiol Rev* 2004;**84**:903-934.
7. Kato J, Tsuruda T, Kita T, Kitamura K, Eto T. Adrenomedullin: a protective factor for blood vessels. *Arterioscler Thromb Vasc Biol* 2005;**25**:2480-2487.
8. Shimosawa T, Shibagaki Y, Ishibashi K, Kitamura K, Kangawa K, Kato S, Ando K, Fujita T. Adrenomedullin, an endogenous peptide, counteracts cardiovascular damage. *Circulation* 2002;**105**:106-111.
9. Shindo T, Kurihara Y, Nishimatsu H, Moriyama N, Kakoki M, Wang Y, Imai Y, Ebihara A, Kuwaki T, Ju KH, Minamino N, Kangawa K, Ishikawa T, Fukuda M, Akimoto Y, Kawakami H, Imai T, Morita H, Yazaki Y, Nagai R, Hirata Y, Kurihara H. Vascular abnormalities and elevated blood pressure in mice lacking adrenomedullin gene. *Circulation* 2001;**104**:1964-1971.
10. Iimuro S, Shindo T, Moriyama N, Amaki T, Niu P, Takeda N, Iwata H, Zhang Y,

Ebihara A, Nagai R. Angiogenic effects of adrenomedullin in ischemia and tumor growth. *Circ Res* 2004;**95**:415-423.

11. Okumura H, Nagaya N, Itoh T, Okano I, Hino J, Mori K, Tsukamoto Y, Ishibashi-Ueda H, Miwa S, Tambara K, Toyokuni S, Yutani C, Kangawa K. Adrenomedullin infusion attenuates myocardial ischemia/reperfusion injury through the phosphatidylinositol 3-kinase/Akt-dependent pathway. *Circulation* 2004;**109**:242-248.
12. Kataoka Y, Miyazaki S, Yasuda S, Nagaya N, Noguchi T, Yamada N, Morii I, Kawamura A, Doi K, Miyatake K, Tomoike H, Kangawa K. The first clinical pilot study of intravenous adrenomedullin administration in patients with acute myocardial infarction. *J Cardiovasc Pharmacol* 2010;**56**:413-419.
13. Maki T, Ihara M, Fujita Y, Nambu T, Miyashita K, Yamada M, Washida K, Nishio K, Ito H, Harada H, Yokoi H, Arai H, Itoh H, Nakao K, Takahashi R, Tomimoto H. Angiogenic and vasoprotective effects of adrenomedullin on prevention of cognitive decline after chronic cerebral hypoperfusion in mice. *Stroke* 2011;**42**:1122-1128.
14. Maki T, Ihara M, Fujita Y, Nambu T, Harada H, Ito H, Nakao K, Tomimoto H, Takahashi R. Angiogenic roles of adrenomedullin through vascular endothelial growth factor induction. *Neuroreport* 2011;**22**:442-447.
15. Iesato Y, Toriyama Y, Sakurai T, Kamiyoshi A, Ichikawa-Shindo Y, Kawate H, Yoshizawa T, Koyama T, Uetake R, Yang L, Yamauchi A, Tanaka M, Igarashi K, Murata T, Shindo T. Adrenomedullin-RAMP2 system is crucially involved in retinal angiogenesis. *Am J Pathol* 2013;**182**:2380-2390.
16. Martinez A, Vos M, Guedez L, Kaur G, Chen Z, Garayoa M, Pio R, Moody T, Stetler-Stevenson WG, Kleinman HK, Cuttitta F. The effects of adrenomedullin overexpression in breast tumor cells. *J Natl Cancer Inst* 2002;**94**:1226-1237.
17. Rocchi P, Boudouresque F, Zamora AJ, Muracciole X, Lechevallier E, Martin PM, Ouafik L. Expression of adrenomedullin and peptide amidation activity in human prostate cancer and in human prostate cancer cell lines. *Cancer Res* 2001;**61**:1196-1206.

18. Forneris M, Gottardo L, Albertin G, Malendowicz LK, Nussdorfer GG. Expression and function of adrenomedullin and its receptors in Conn's adenoma cells. *Int J Mol Med* 2001;**8**:675-679.

19. McLatchie LM, Fraser NJ, Main MJ, Wise A, Brown J, Thompson N, Solari R, Lee MG, Foord SM. RAMPs regulate the transport and ligand specificity of the calcitonin-receptor-like receptor. *Nature* 1998;**393**:333-339.

20. Parameswaran N, Spielman WS. RAMPs: The past, present and future. *Trends Biochem Sci* 2006;**31**:631-638.

21. Ichikawa-Shindo Y, Sakurai T, Kamiyoshi A, Kawate H, Iinuma N, Yoshizawa T, Koyama T, Fukuchi J, Iimuro S, Moriyama N, Kawakami H, Murata T, Kangawa K, Nagai R, Shindo T. The GPCR modulator protein RAMP2 is essential for angiogenesis and vascular integrity. *J Clin Invest* 2008;**118**:29-39.

22. Koyama T, Ochoa-Callejero L, Sakurai T, Kamiyoshi A, Ichikawa-Shindo Y, Iinuma N, Arai T, Yoshizawa T, Iesato Y, Lei Y, Uetake R, Okimura A, Yamauchi A, Tanaka M, Igarashi K, Toriyama Y, Kawate H, Adams RH, Kawakami H, Mochizuki N, Martinez A, Shindo T. Vascular endothelial adrenomedullin-RAMP2 system is essential for vascular integrity and organ homeostasis. *Circulation* 2013;**127**:842-853.

23. Ebos JM, Lee CR, Cruz-Munoz W, Bjarnason GA, Christensen JG, Kerbel RS. Accelerated metastasis after short-term treatment with a potent inhibitor of tumor angiogenesis. *Cancer Cell* 2009;**15**:232-239.

24. Paez-Ribes M, Allen E, Hudock J, Takeda T, Okuyama H, Vinals F, Inoue M, Bergers G, Hanahan D, Casanovas O. Antiangiogenic therapy elicits malignant progression of tumors to increased local invasion and distant metastasis. *Cancer Cell* 2009;**15**:220-231.

25. Sorensen I, Adams RH, Gossler A. DLL1-mediated Notch activation regulates endothelial identity in mouse fetal arteries. *Blood* 2009;**113**:5680-5688.

26. Saiki I, Iida J, Murata J, Ogawa R, Nishi N, Sugimura K, Tokura S, Azuma I. Inhibition

of the metastasis of murine malignant melanoma by synthetic polymeric peptides containing core sequences of cell-adhesive molecules. *Cancer Res* 1989;**49**:3815-3822.

27. Reutershan J, Morris MA, Burcin TL, Smith DF, Chang D, Saprito MS, Ley K. Critical role of endothelial CXCR2 in LPS-induced neutrophil migration into the lung. *J Clin Invest* 2006;**116**:695-702.

28. Ishiguro T, Nakajima M, Naito M, Muto T, Tsuruo T. Identification of genes differentially expressed in B16 murine melanoma sublines with different metastatic potentials. *Cancer Res* 1996;**56**:875-879.

29. Lin F, Wang N, Zhang TC. The role of endothelial-mesenchymal transition in development and pathological process. *IUBMB Life* 2012;**64**:717-723.

30. Hiratsuka S, Watanabe A, Aburatani H, Maru Y. Tumour-mediated upregulation of chemoattractants and recruitment of myeloid cells predetermines lung metastasis. *Nat Cell Biol* 2006;**8**:1369-1375.

31. Hiratsuka S, Watanabe A, Sakurai Y, Akashi-Takamura S, Ishibashi S, Miyake K, Shibuya M, Akira S, Aburatani H, Maru Y. The S100A8-serum amyloid A3-TLR4 paracrine cascade establishes a pre-metastatic phase. *Nat Cell Biol* 2008;**10**:1349-1355.

32. Hiratsuka S, Ishibashi S, Tomita T, Watanabe A, Akashi-Takamura S, Murakami M, Kijima H, Miyake K, Aburatani H, Maru Y. Primary tumours modulate innate immune signalling to create pre-metastatic vascular hyperpermeability foci. *Nat Commun* 2013;**4**:1853.

33. Zecchin A, Borgers G, Carmeliet P. Endothelial cells and cancer cells: metabolic partners in crime? *Curr Opin Hematol* 2015;**22**:234-242.

34. Yamauchi A, Sakurai T, Kamiyoshi A, Ichikawa-Shindo Y, Kawate H, Igarashi K, Toriyama Y, Tanaka M, Liu T, Xian X, Imai A, Zhai L, Owa S, Arai T, Shindo T. Functional differentiation of RAMP2 and RAMP3 in their regulation of the vascular system. *J Mol Cell Cardiol* 2014;**77**:73-85.

35. Zeisberg EM, Potenta S, Xie L, Zeisberg M, Kalluri R. Discovery of endothelial to

mesenchymal transition as a source for carcinoma-associated fibroblasts. *Cancer Res* 2007;**67**:10123-10128.

36. Garcia J, Sandi MJ, Cordelier P, Binetruy B, Pouyssegur J, Iovanna JL, Tournaire R. Tie1 deficiency induces endothelial-mesenchymal transition. *EMBO reports* 2012;**13**:431-439.

37. Wang R, Chadalavada K, Wilshire J, Kowalik U, Hovinga KE, Geber A, Fligelman B, Leversha M, Brennan C, Tabar V. Glioblastoma stem-like cells give rise to tumour endothelium. *Nature* 2010;**468**:829-833.

38. Foell D, Wittkowski H, Vogl T, Roth J. S100 proteins expressed in phagocytes: a novel group of damage-associated molecular pattern molecules. *J Leukoc Biol* 2007;**81**:28-37.

39. Coussens LM, Werb Z. Inflammation and cancer. *Nature* 2002;**420**:860-867.

40. Tomita T, Sakurai Y, Ishibashi S, Maru Y. Imbalance of Clara cell-mediated homeostatic inflammation is involved in lung metastasis. *Oncogene* 2011;**30**:3429-3439.

41. Ashizuka S, Inatsu H, Kita T, Kitamura K. Adrenomedullin Therapy in Patients with Refractory Ulcerative Colitis: A Case Series. *Dig Dis Sci* 2015.

Figure Legends

Fig. 1.

Transplanted tumor angiogenesis and growth are suppressed in drug-inducible endothelial cell-specific RAMP2 knockout (DI-E-RAMP2-/-) mice

(A) Representative image of sarcoma 180 tumors removed from control and DI-E-RAMP2-/- mice. (B) Representative images of B16F10 melanomas showing tumor self-destruction in DI-E-RAMP2-/- mice. Scale bars in (A), (B) = 1 cm. (C) Tumor weights of S180 and B16F10 in control and DI-E-RAMP2-/- mice. For sarcoma 180, n = 11 in both groups. For B16F10 melanoma, n = 10 for control and n = 8 for DI-E-RAMP2-/-. Bars are the mean ± SEM. *P<0.05, **P<0.01. (D) Histological evaluation of angiogenesis within B16F10 melanomas. Capillarization within a transplanted B16F10 melanoma from a control and DI-E-RAMP2-/- mouse is revealed by immunostaining for CD31 (red), an endothelial cell marker, and DAPI (blue), a nuclear marker. Scale bars = 50 μm. (E) Ratios of CD31-positive vascular area / DAPI-positive area in the B16F10 melanomas from control and DI-E-RAMP2-/- mice. An average of 10 microscopic fields per tumor were used. n = 6 in both groups. Bars are the mean ± SEM. *P<0.05. (F) Quantitative real-time PCR analysis of AM, RAMP2, and angiogenesis markers in B16F10 melanoma. n = 4~5. (G), (H) Matrigel plug assay of in vivo angiogenesis. (G) Image of transplanted Matrigel showing reduced angiogenesis in DI-E-RAMP2-/- mice. Scale bars = 2 mm. (H) Fluorescence immunostaining of Matrigel sections showing the vascular front: red, CD31 (endothelial cell marker); green, αSMA (smooth muscle cell marker); blue, DAPI. Hypoplasia of the tip cells is apparent in DI-E-RAMP2-/- mice (compare areas indicated by the arrows). Scale bars = 100 μm.

Fig. 2.

Lung metastasis is enhanced in DI-E-RAMP2-/- mice

(A) Representative images of spontaneous lung metastases arising from primary B16BL6

melanomas transplanted into hindlimb footpads 7 weeks before the analysis. (B) Incidence of spontaneous lung metastasis from a primary lesion (footpad). Bars show the percentage of mice exhibiting metastasis. ****P<0.0001 (χ2-test). n = 12 for control and n =13 for DI-E-RAMP2-/-. (C) Number of metastatic lesions per lung. n = 8 in both groups. Bars are the mean ± SEM. (D) Lung metastasis was confirmed by Fontana-Masson staining (representing melanin pigment). Scale bars =100 μm.

Fig. 3.

Analysis of blood vessel structure in primary B16F10 melanomas

(A) Appearance of a control and DI-E-RAMP2-/- mouse (on day 26 of the induction of RAMP2-deletion). (B) Comparison of body weight in control and DI-E-RAMP2-/- mice. The first day of tamoxifen administration was defined as day 1. Tamoxifen was administered from day 1 to 5 to induce RAMP2-deletion. B16F10 melanoma cells were transplanted subcutaneously into the axillary region on day 8. At both day 8 (before the tumor transplantation) and day 20 (after the tumor transplantation), body weight was significantly higher in DI-E-RAMP2-/- compared with control mice. Day 8: n = 8, Day 20: n = 5 in both groups. Data shown are the mean ± SEM. *P<0.05, **P<0.01. (C) Images of the vasculature in the primary tumor after indocyanine green (ICG) injection. B16F10 melanoma cells were transplanted into the axillary region 2 weeks before this analysis. Vascular structure was visualized 30 min after peritoneal injection of ICG. Scale bars = 200 μm. (D) Electron micrographs of blood vessels in tumors in control and DI-E-RAMP2-/- mice. EC = endothelial cells. Scale bars = 1 μm. (E) Electron micrographs of the endothelial side of the glomerular loop 7 weeks after gene deletion. The endothelial side of the glomerular loop showed a peculiar change; it looked like honeycomb composed of multiple layers of endothelial cells. EC = endothelial cells. Scale bars = 1 μm. (F) TUNEL staining in a section of B16F10 melanoma tissue. Nuclei were counter-stained by methyl green. Vascular lumens within tumors are enclosed by dotted lines. Scale bars = 100 μm. (G) Comparison of the percentage of TUNEL-

positive nuclei in the sections of B16F10 melanoma tissues. n = 5 in both groups. Data shown are the mean ± SEM. *P<0.05

Fig. 4.

Endothelial-mesenchymal transition (EndMT) change was enhanced in DI-E-RAMP2-/- mice

(A) Fluorescent immunostaining of sections of primary B16F10 melanomas transplanted into the axillary region 3 weeks before the analysis: red, CD31 (endothelial cell marker); green, αSMA (smooth muscle cell marker); blue, DAPI. Scale bars = 100 μm. Experiments were repeated 4 times and representative figures are shown. (B) Fluorescent immunostaining of HUVECs co-cultured with B16F10 melanoma cells from tumors transplanted 2 weeks earlier; green, VE-cadherin (endothelial cell marker); red, phalloidin (actin marker); blue, DAPI. Scale bars = 50 μm. Experiments were repeated 4 times and representative figures are shown. (C) Fluorescent immunostaining of HUVECs treated with TGF-β (10 ng/mL) with or without AM (10^{-7} M). Cells were pre-treated with AM or PBS for 24h followed by treatment with TGF-β for an additional 48 h: green, VE-cadherin; red; phalloidin; blue; DAPI. Scale bars = 50 μm. Experiments were repeated 4 times and representative figures are shown. (D) Fluorescent immunostaining of TGF-β-treated (10 ng/mL, 24 h) primary pulmonary endothelial cells from control and DI-E-RAMP2-/- mice: red, FSP-1 (mesenchymal cell marker); green, VE-cadherin (endothelial cell marker); blue; DAPI. Arrows indicate FSP-1-positive cells. Scale bars = 50 μm. Experiments were repeated 5 times and representative figures are shown. (E) Percentages of FSP-1-positive cells per VE-cadherin-positive cells from DI-E-RAMP2-/- and control mice. n = 5 for both. Bars are the mean ± SEM. **P<0.01.

Fig. 5.

Evaluation of pre-metastatic niche formation in the lung after RAMP2 deletion

(A) H&E staining of lung after induction of RAMP2 deletion for 26 days (without tumor

transplantation). RAMP2-deficiency enhanced interstitial edema. Scale bars = 200 μm. (B) Electron micrographs showing pulmonary endothelial cells (arrows) after 19 days of RAMP2 deletion. Scale bars = 1 μm. Pulmonary endothelial cells of DI-E-RAMP2-/- were deformed and extended into the vascular lumen with numerous protrusions on their surface. Experiments were repeated 4 times and representative figures are shown. (C) Quantitative real-time PCR analysis of RAMP2, VE-cadherin, and actin expression in the lung tissue on day 26 of RAMP2 deletion. n = 5~8. Bars are the mean ± SEM. **P<0.01, *P<0.05.

Fig. 6.

RAMP2 deletion increases pulmonary inflammation, oxidative stress, and tumor cell chemotactic factors in the lung

(A) Fluorescent immunostaining of lung sections on day 8 of RAMP2 deletion: green, F4/80 (macrophage marker); blue. DAPI. Scale bars = 50 μm. (B) Immunohistochemical staining for 4HNE (oxidative stress marker) in lung sections. Scale bars = 100 μm. (C) Quantitative real-time PCR analysis showing expression of the indicated inflammatory cytokines and NADPH oxidase subunits in control and DI-E-RAMP2-/- lungs on the indicated day. n = 4~6. Bars are the mean ± SEM. *P<0.05. (D) Immunohistochemical staining for S100A8 in lung tissues from control and DI-E-RAMP2-/- mice on day 26 of RAMP2 deletion. Scale bars = 50 μm. (E) Quantitative real-time PCR analysis of S100A8 and S100A9 expression in lung on day 26 of RAMP2 deletion. n = 5~8. Bars are the mean ± SEM. *P<0.05.

Fig. 7.

Overexpression of RAMP2 in vascular endothelial cells suppresses metastasis

(A) Fluorescence micrographs showing adhesion of B16F10 melanoma cells to control and RAMP2-overexpressing (RAMP2 O/E) EAhy926 endothelial cells: red, Ds-Red-expressing B16F10 melanoma cells; blue, DAPI. Scale bars = 200 μm. (B) Relative level of B16F10 melanoma cell adhesion to control and RAMP2 O/E endothelial cells (EC). Shown are the Ds-

Red-positive / DAPI-positive cell ratios. n = 9 for each. Bars are the mean ± SEM. **P<0.01. (C) Representative images of spontaneous lung metastasis. The primary B16BL6 melanoma cells were transplanted into hindlimb footpads 7 weeks before the observation. (D) Kaplan-Meier curve comparing survival time between E-RAMP2 Tg (n = 7) and WT mice (n = 8). B16BL6 melanoma cells were transplanted into footpads (time 0), and the primary lesions were then resected after 3 weeks (dotted vertical line).

Fig. 8.

The role of AM-RAMP2 system in tumor angiogenesis and metastasis

In cancer, pathological angiogenesis promotes primary tumor growth, while endothelial-mesenchymal transition (EndMT) in tumor vessels and the environment within distant organs (pre-metastatic niche) increase the occurrence of metastasis. Controlling vascular integrity is thus expected to be a therapeutic target of cancers. Endothelial AM-RAMP2 system regulates vascular integrity and suppresses tumor metastasis, and it could be a novel therapeutic target.

Primers and probes used for quantitative real-time RT-PCR

AM Forward	CTACCGCCAGAGCATGAACC	TGF-β Forward	CCCGAAGCGGACTACTATGC
AM Reverse	GAAATGTGCAGGTCCCGAA	TGF-β Reverse	TAGATGGCGTTGTTGCGGT
AM Probe	CCCGCAGCAATGGATGCCG	p67phox Forward	CAGACCCAAAACCCCAGAAA
RAMP2 Forward	GCAGCCCACCTTCTCTGATC	p67phox Reverse	AAAGCCAAACAATACGCGGT
RAMP2 Reverse	AACGGGATGAGGCAGATGG	p47phox Forward	ATCCTATCTGGACCCCTTGA
RAMP2 Probe	CCCAGAGGATGTGCTCCTGGCCAT	p47phox Reverse	CACCTGCGTAGTTGGGATCC
VEGF-A Forward	CATCTTCAAGCCGTCCTGTGT	ICAM-1 Forward	CCTAAAATGACCTGCAGACGG
VEGF-A Reverse	CTCCAGGGCTTCATCGTTACA	ICAM-1 Reverse	TTTGACAGACTTCACCACCCC
VEGFR-2 Forward	CATCTTCAAGCCGTCCTGTGT	VCAM-1 Forward	CCCTGAATACAAAACGATCGC
VEGFR-2 Reverse	TCATTGCCCGCTTAACG	VCAM-1 Reverse	CAGCCCGTAGTGCTGCAAG
CD31 Forward	CTGCAGGCATCGGCAAA	Actin Forward	ACTGGGACGACATGGAAAAGAT
CD31 Reverse	GCATTTCGCACACCTGGAT	Actin Reverse	CACTATTTCTATAACGAGCTTCGTGTGGCC
IL-6 Forward	TGAATTGGATGGTCTTGGTCC	S100A8 Forward	TGAGCAACCTCATTGATGTCTACC
IL-6 Reverse	TGAATTGGATGGTCTTGGTCC	S100A8 Reverse	ATGCCACACCCACTTTTATCACC
TNF-α Forward	ACGGCATGGATCAAAGAC	S100A9 Forward	GAAGAAAGAGAAGAGAAATGAAGCC
TNF-α Reverse	AGATAGCAAATCGGCTGACG	S100A9 Reverse	CTTGCCATCAGCATCATACACTCC
VE-cadherin Forward	GGTGCCAAAGACCCTGAC	SAA3 Forward	GTTGACAGCCAAAGATGGGT
VE-cadherin Reverse	ACTGGTCTTGCGGATGGAGT	SAA3 Reverse	CCCGAGCATGGAAGTATTTG

Table. 1.

Top 10 genes upregulated in the lung of DI-E-RAMP2-/- (vs. control)

clca3	NM_017474	chloride channel calcium activated 3 [Source:MarkerSymbol;Acc:MGI:1346342]	6.91
Irg1	XM_127883	immunoresponsive gene 1 [Source:MarkerSymbol;Acc:MGI:103206]	6.79
Ear11	NM_053113	eosinophil-associated, ribonuclease A family, member 11 [Source:MarkerSymbol;Acc:MGI:1890465]	6.26
Saa3	NM_011315	serum amyloid A 3 [Source:MarkerSymbol;Acc:MGI:98223]	5.40
Cd300e	NM_172050	CD300e antigen [Source:MarkerSymbol;Acc:MGI:2387602]	5.09
Treml4	NM_172623	triggering receptor expressed on myeloid cells-like 4 [Source:MarkerSymbol;Acc:MGI:1923239]	5.07
Chi3l4	NM_145126	chitinase 3-like 4 [Source:MarkerSymbol;Acc:MGI:1341098]	4.75
Il10	NM_01548	interleukin 10 [Source:MarkerSymbol;Acc:MGI:96537]	4.72
Mmp12	NM_008605	matrix metallopeptidase 12 [Source:MarkerSymbol;Acc:MGI:97005]	4.67
Il6	NM_031168	interleukin 6 [Source:MarkerSymbol;Acc:MGI:96559]	4.63

Table. 2.

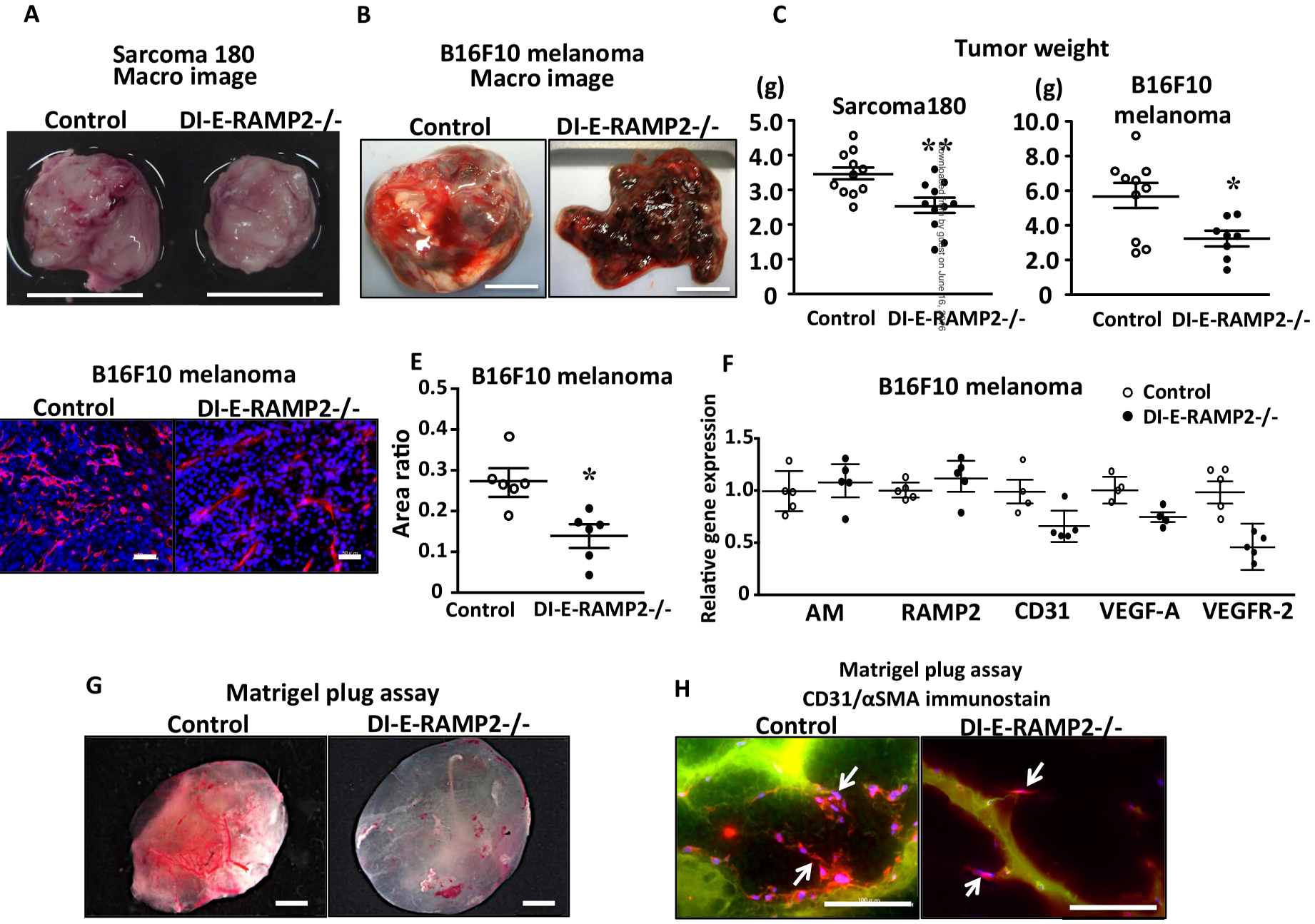

Fig. 1.

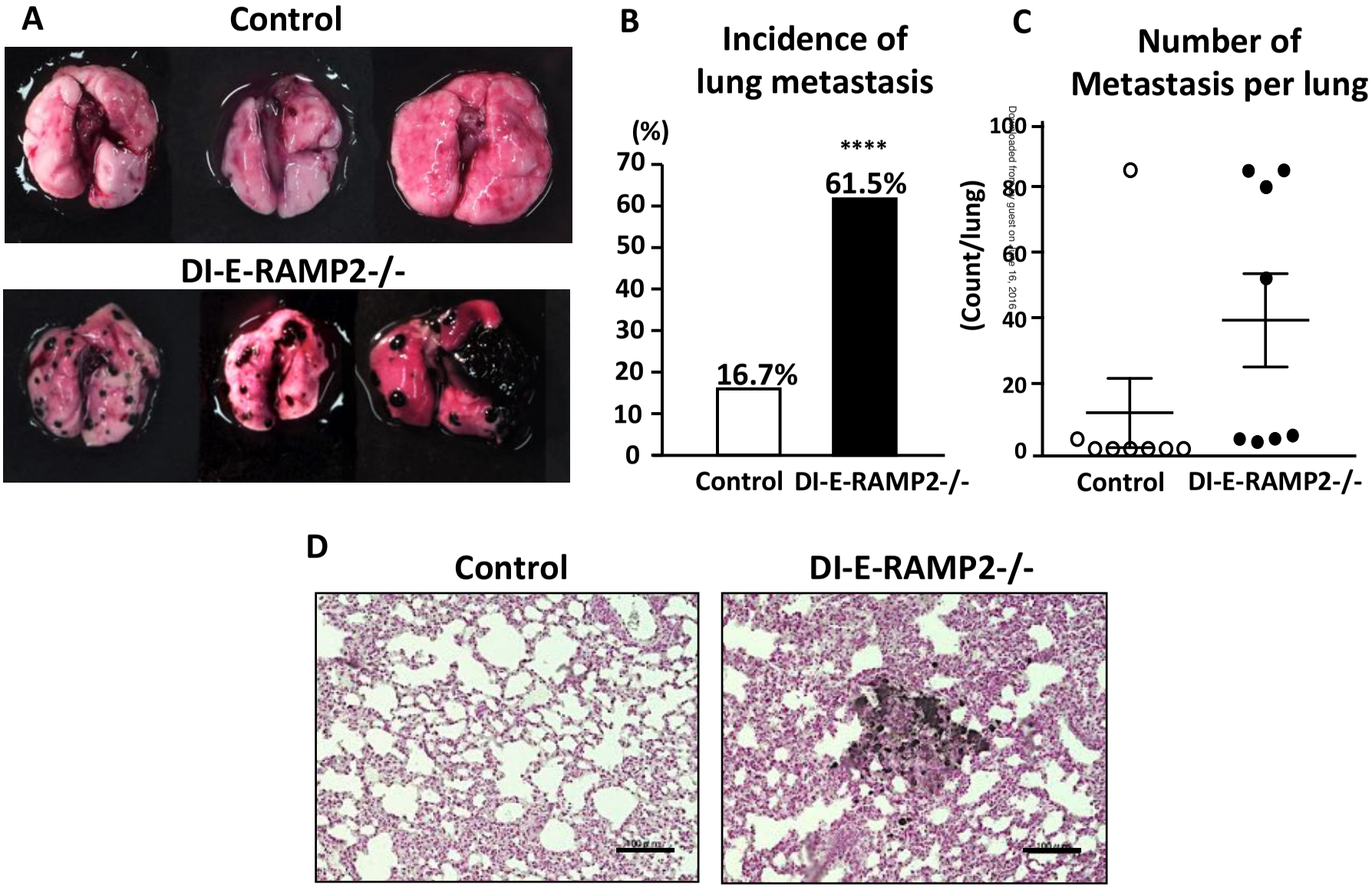

Fig. 2.

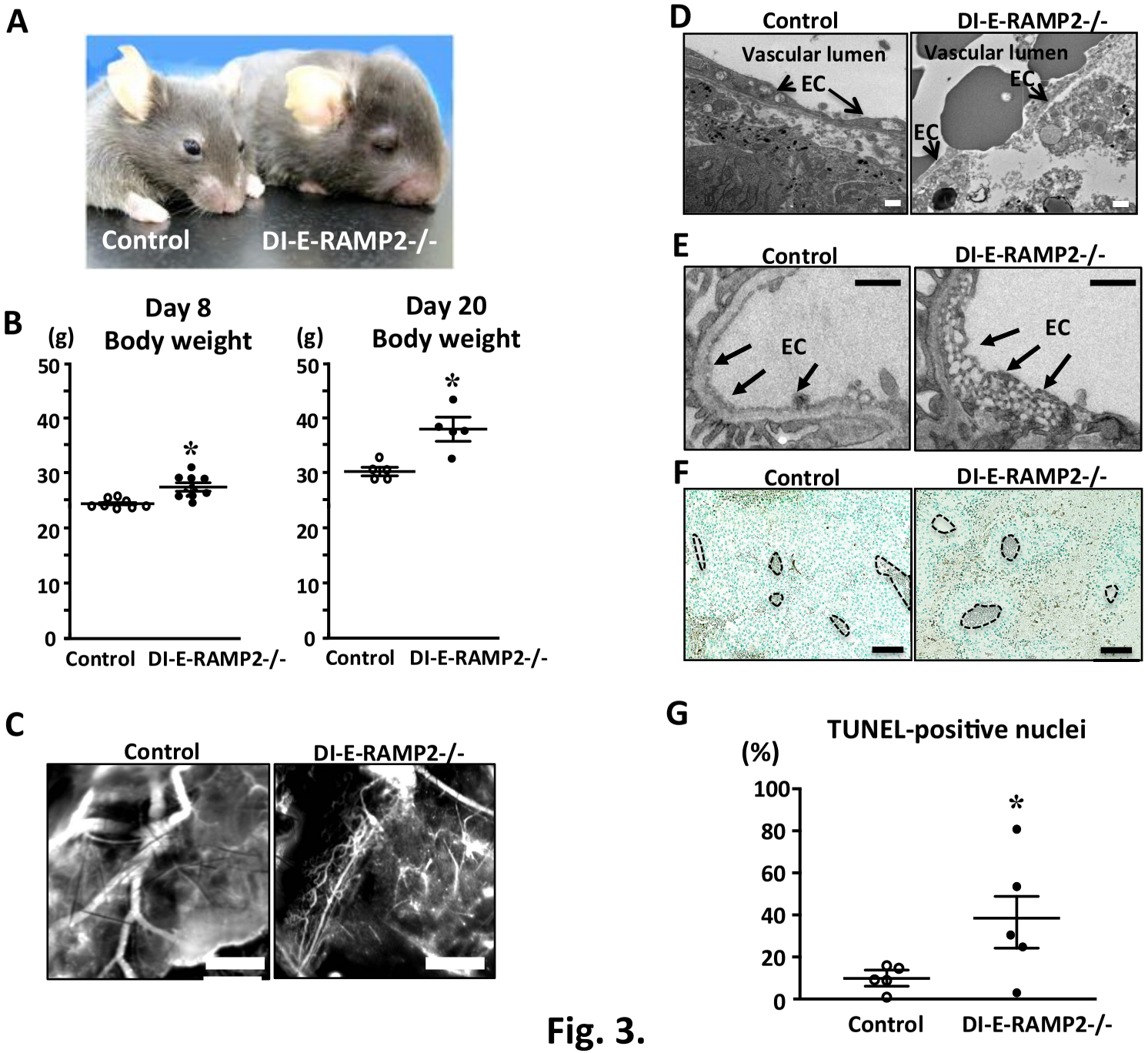
A
Control
DI-E-RAMP2-/-
B
Day 8
Body weight
(g)
50
40
30
20
10
0
Control
DI-E-RAMP2-/-
Day 20
Body weight
(g)
50
40
30
20
10
0
Control
DI-E-RAMP2-/-
C
Control
DI-E-RAMP2-/-
D
Control
DI-E-RAMP2-/-
Vascular lumen
EC
Vascular lumen
EC
EC
E
Control
DI-E-RAMP2-/-
EC
EC
F
Control
DI-E-RAMP2-/-
G
TUNEL-positive nuclei
(%)
100
80
60
40
20
0
Control
DI-E-RAMP2-/-

Fig. 3.

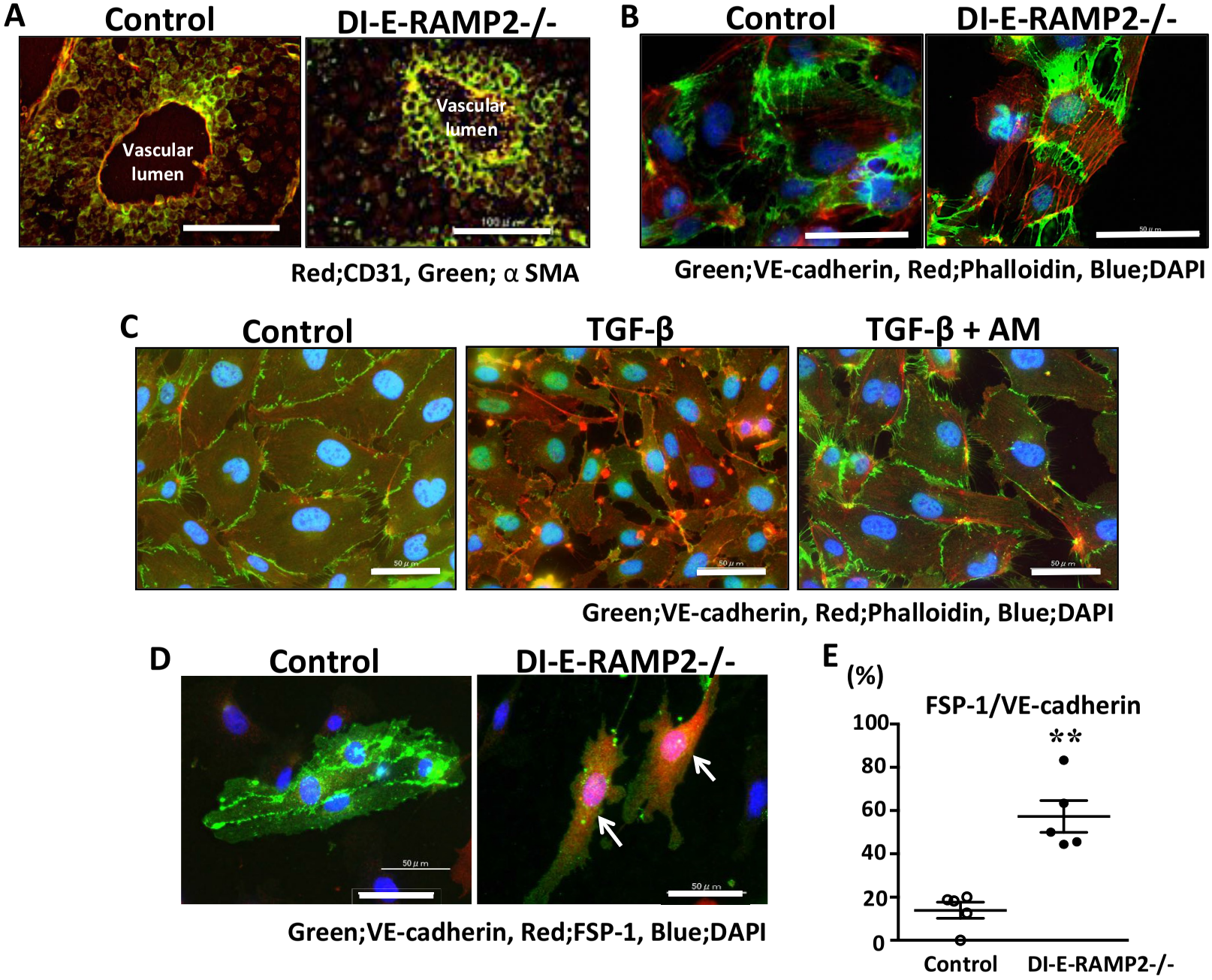

Fig. 4.

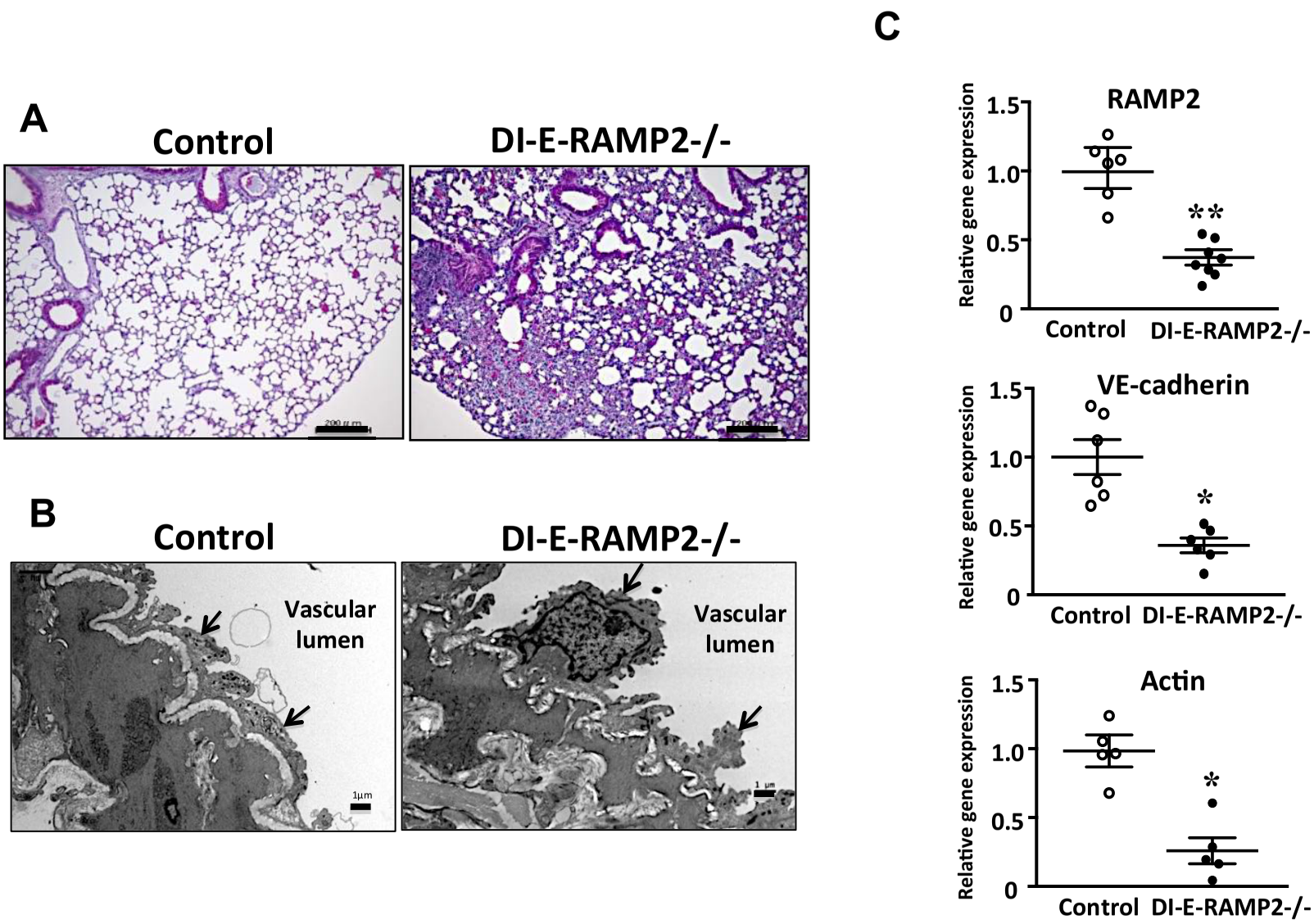

Fig. 5.

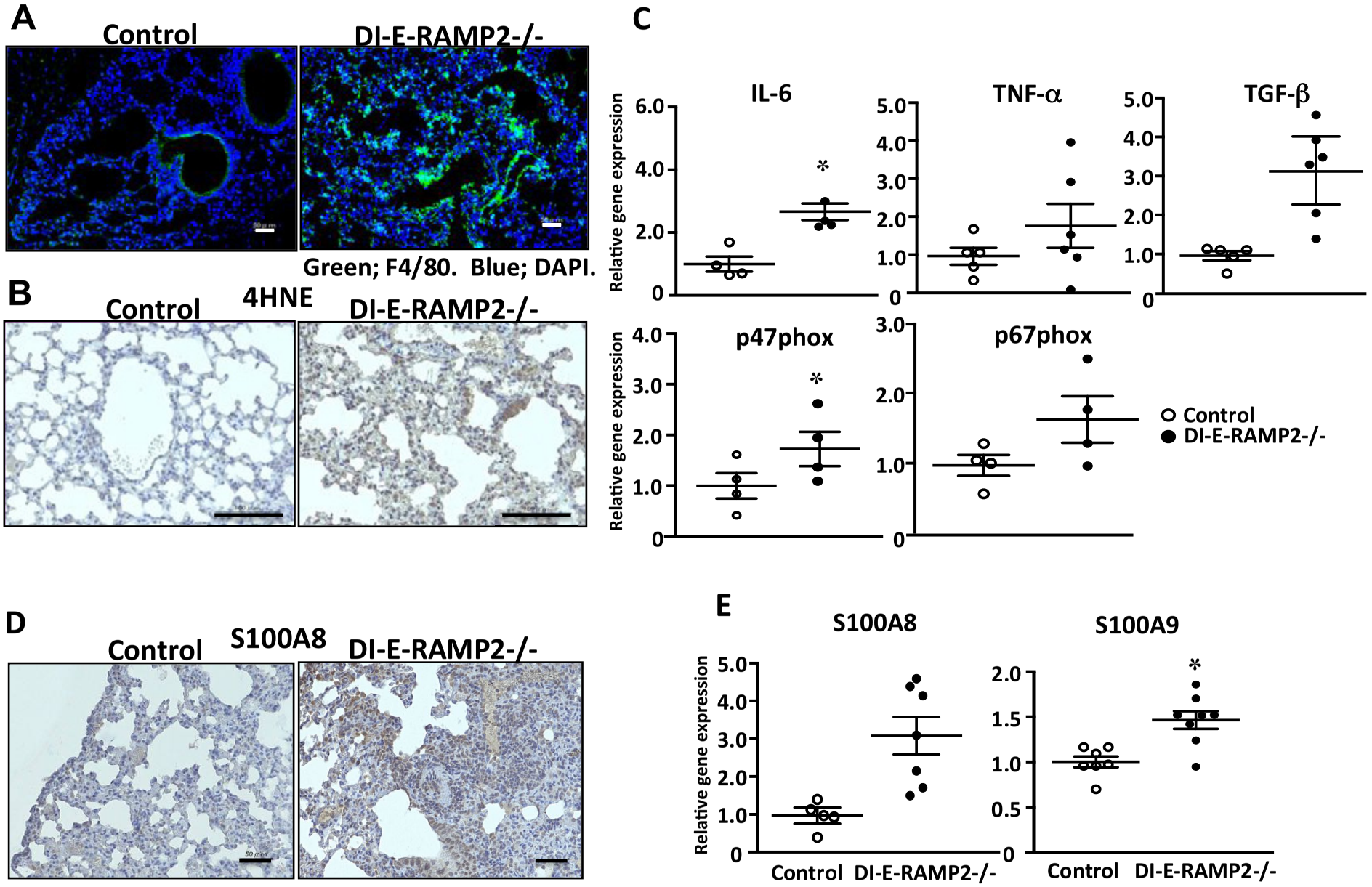
A
Control
DI-E-RAMP2-/-
Green; F4/80. Blue; DAPI.
B
Control
4HNE
DI-E-RAMP2-/-
C
IL-6
TNF-α
TGF-β
p47phox
p67phox
Relative gene expression
Control
DI-E-RAMP2-/-
D
Control
S100A8
DI-E-RAMP2-/-
E
S100A8
S100A9
Relative gene expression
Control
DI-E-RAMP2-/-

Fig. 6.

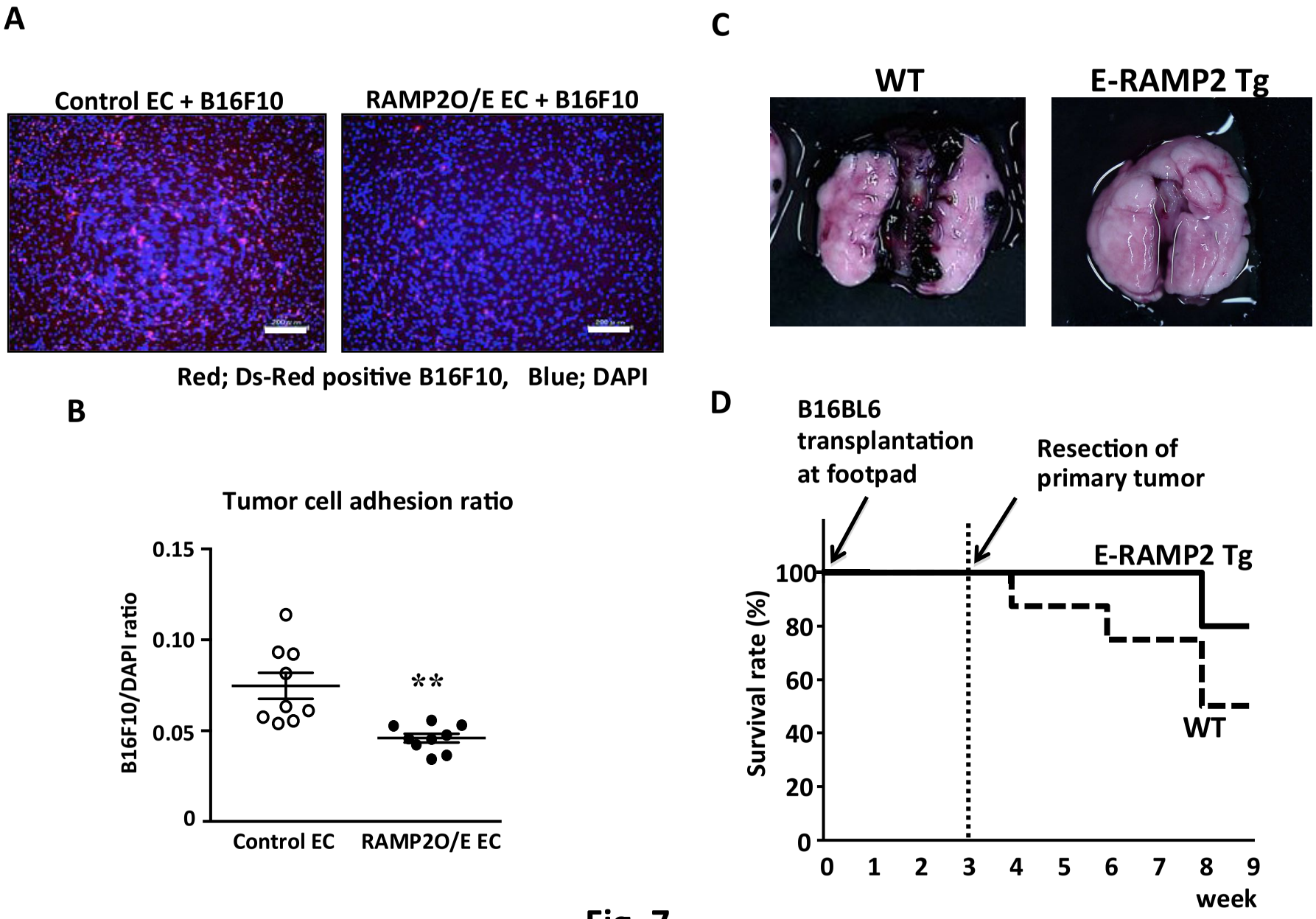

Fig. 7.

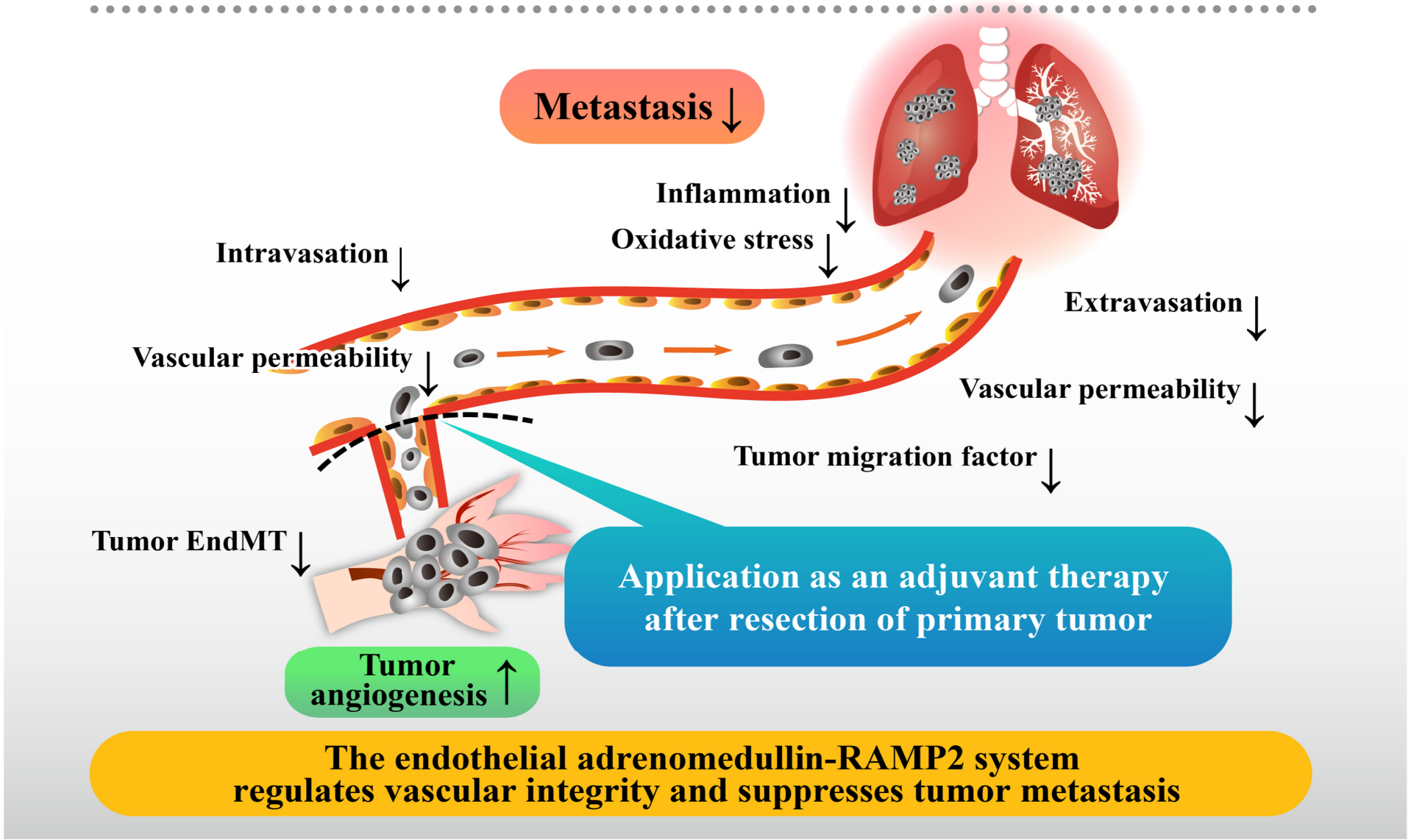
The role of adrenomedullin-RAMP2 system in tumor angiogenesis and metastasis
Metastasis ↓
Inflammation ↓
Oxidative stress ↓
Intravasation ↓
Extravasation ↓
Vascular permeability ↓
Vascular permeability ↓
Tumor migration factor ↓
Tumor EndMT ↓
Application as an adjuvant therapy after resection of primary tumor
Tumor angiogenesis ↑
The endothelial adrenomedullin-RAMP2 system regulates vascular integrity and suppresses tumor metastasis

Fig. 8.